Mapping of Macular Substructures with Optical Coherence Tomography for Glaucoma Diagnosis

*Ou Tan, PhD, Gisèle Li, MD, Ake Tzu-Hui Lu, PhD, Rohit Varma, MD, MPH, David Huang, MD, PhD, Advanced Imaging for Glaucoma Study Group**

Purpose: To use optical coherence tomography (OCT) to identify the specific retinal layers and macular regions damaged in glaucoma.

Design: Observational cross-sectional study.

Participants: One hundred forty-nine participants in the Advanced Imaging for Glaucoma Study, divided into 3 groups: normal (N) perimetric glaucoma (PG), and glaucoma suspect and preperimetric glaucoma (GSPPG) with 44, 73, and 29 persons, respectively.

Methods: The Zeiss Stratus OCT system (Carl Zeiss Meditec, Inc., Dublin, CA) was used to map the macula over a 6-mm diameter and to scan the circumpapillary nerve fiber layer (cpNFL). The macular OCT images were exported for automatic segmentation using software developed by the authors. The thickness of the macular nerve fiber layer (mNFL), ganglion cell layer (mGCL), inner plexiform layer (mIPL), inner nuclear layer (mINL), outer retinal layer (mORL), and total retinal thickness were measured. Thickness measurements of GSPPG and PG eyes were compared with those of N eyes. The ability to differentiate between GSPPG and PG eyes against N eyes was assessed by fractional loss, standardized deviation, and the area under the receiver operating characteristic curve.

Main Outcome Measures: Area-weighted average thicknesses of retinal sublayers in the macula.

Results: The mNFL, mGCL, mIPL, and mINL were significantly ($P<0.001$) thinner in both the GSPPG and PG eyes than in the N eyes. In PG eyes, mNFL, mGCL, and mIPL thinning was most severe (approximately 20%), mINL thinning was intermediate (7%), and mORL thinning was minimal (3%). The repeatability (coefficient of variation and intraclass correlation) of thickness measurements was improved by combining the mNFL, mGCL, and mIPL measurements as the inner retinal layer (mIRL). The mIRL was the best macular parameter for glaucoma diagnosis and had discriminant power comparable with that of the cpNFL. The fractional loss of mIRL thickness was most severe in the inferior perifoveal region for both the PG and GSPPG groups.

Conclusions: Glaucoma leads to thinning of the mNFL, mGCL, mIPL, and mINL, even before detectable visual field changes occur. A combination of the 3 innermost layers seems to provide optimal glaucoma detection. Increasing the sampling of peripheral macula with a new OCT scan pattern may improve glaucoma diagnosis further. *Ophthalmology 2008;115:949–956 © 2008 by the American Academy of Ophthalmology.*

Glaucoma is an optic neuropathy characterized by an irreversible loss of neural tissue and visual field function. Early detection of the disease or its progression is important in determining the required intervention to prevent irreversible damage and visual loss. The earliest observable defect in glaucoma is atrophy of the nerve fiber layer (NFL).[1] Loss of the disc rim in the optic nerve head also has been shown to precede visual field (VF) loss.[2–4]

Advanced imaging systems such as optical coherence tomography (OCT), scanning laser polarimetry, and scanning laser tomography can measure objectively both retinal NFL thickness and optic disc contour.

The macular region does not undergo clinically observable change with glaucoma. But the development of more sensitive measurement technology has sparked interest in investigating this area for glaucoma diagnosis. Zeimer[5–7] hypothesized that macular thickness was important because the retinal ganglion cell layer consists of the cell bodies of retinal nerve fibers, and ganglion cell bodies are represented disproportionately in the macula. The macula is the only

Originally received: February 15, 2007.
Final revision: July 27, 2007.
Accepted: August 6, 2007.
Available online: November 5, 2007. Manuscript no. 2007-211.

From the Doheny Eye Institute, University of Southern California, Los Angeles, California.

Supported by the National Institutes of Health, Bethesda, Maryland (grant nos. R01 EY013516, P30 EY03040), and Research to Prevent Blindness, Inc., New York, New York.

Dr Huang receives patent royalty and research grants from Carl Zeiss Meditec, Inc.

Correspondence to Ou Tan, PhD, Doheny Eye Institute, 1355 San Pablo Street, DVRC160-C, Los Angeles, CA 90033.

*A complete list of Study Group members is available at http://www.AIGStudy.net.

ISSN 0161-6420/08/$–see front matter
doi:10.1016/j.ophtha.2007.08.011

area where the ganglion cell layer is more than 1 cell layer thick.[5]

Several clinical studies have shown that the circumpapillary NFL (cpNFL) thickness is a more sensitive detector of glaucoma than macular retinal thickness.[8–11] However, this advantage may be the result of the inherent limitations of macular measurements. The current macular scanning pattern on the Stratus OCT system (Carl Zeiss Meditec, Inc., Dublin, CA; software version 4.0) measures diameters of 6 mm (20.8°), whereas glaucoma usually affects more peripheral regions, causing the typical visual field defect patterns such as the nasal step and arcuate defects. Furthermore, measuring the entire retinal thickness may decrease the specificity of glaucoma diagnosis, because only the inner retinal layers should be affected, whereas the outer layers merely increase measurement variability.

Improvements in the resolution of imaging technologies have made segmentation (delineation of boundaries) and measurement of individual retinal layers possible. The retinal thickness analyzer developed by Asrani and Zeimer[12] has a repeatability of 30 μm. The earliest commercial OCT retinal scanners, OCT1 and OCT2, had 12 to 16 μm full-width at half-maximum axial resolution. The latest system, the Stratus (a.k.a., OCT3), has a higher resolution of 9 to 10 mm full-width at half-maximum in tissue and permits visualization of individual retinal layers.[13] Even higher resolution currently is possible with ultrahigh-resolution OCT, which has demonstrated an axial resolution of approximately 3 μm.[14]

A macular segmentation algorithm for OCT was developed by Ishikawa et al.[15] Their results indicate that the macular nerve fiber layer (mNFL) and inner retinal complex (ganglion cell, inner plexiform, and inner nuclear layers) thickness are comparable with cpNFL thickness in discriminating normal eyes from glaucomatous eyes.

The objectives of this study were: (1) to identify the specific retinal layers involved in glaucoma; (2) to identify the areas of macula most affected by glaucoma; and (3) to formulate a strategy to optimize OCT macular scanning for detecting glaucomatous damage.

Patients and Methods

Study Participants

Participants in the prospective Advanced Imaging for Glaucoma Study between 2003 and 2005 were included. These participants were classified into 3 groups: normal (N), perimetric glaucoma (PG), or glaucoma suspect and preperimetric glaucoma (GSPPG). The Advanced Imaging for Glaucoma Study is a longitudinal study, but only the data from the baseline visit were used for this study. The eligibility criteria for the 3 groups are described below briefly.

Participants were assigned to the N group if both eyes had intraocular pressure (IOP) of less than 21 mmHg, normal VFs as obtained using the Humphrey Swedish interactive threshold algorithm 24-2 (Humphrey Instruments, San Leandro, CA; defined as having a mean deviation [MD] and pattern standard deviation [PSD] within 95% limits of the normal reference and glaucoma hemifield test results within 97% limits), a central corneal thickness (CCT) of more than 500 μm, an open anterior chamber angle, a normal-appearing optic nerve head, a normal nerve fiber layer, and the patient had no history of chronic ocular or systemic corticosteroid use.

Participants were classified as PG if at least 1 eye fulfilled the following criteria: glaucomatous (abnormal) VF loss (defined as a PSD [$P<0.05$] or glaucoma hemifield test results [$P<0.01$] outside normal limits in a consistent pattern on both qualifying VFs) and optic nerve head changes such as diffuse or localized rim thinning, disc (splinter) hemorrhage, notch in the rim, vertical cup-to-disc ratio more than the fellow eye by more than 0.2, or previous photographic documentation of progressive excavation of the disc, progressive thinning of the neuroretinal rim or NFL defects visible on slit-lamp biomicroscopy, or progressive loss of NFL.

Participants assigned to the GSPPG group were those identified as being glaucoma suspects or having preperimetric glaucoma. To be labeled as GSPPG, an eye had to have 1 or more of the following risk factors or abnormalities: ocular hypertension (defined as IOP of 24 mmHg or more in 1 eye and IOP of 22 mmHg or more in the fellow eye), optic nerve head or NFL defects visible on slit-lamp biomicroscopy or stereo color fundus photography as defined for the PG group, and a fellow eye that met the eligibility criteria for the PG group. The VFs of eyes in the GSPPG group did not meet the eligibility criteria for the PG group.

Patients with (1) a best-corrected visual acuity worse than 20/40, (2) age less than 40 or more than 79 years, or (3) a refractive error of more than 3.00 diopters (D) or <-7.00 D were excluded. Patients also were excluded if they had diabetic retinopathy or other diseases that could cause visual field loss or optic disc abnormalities or if they had undergone previous intraocular surgery other than an uncomplicated cataract extraction with posterior chamber IOL implantation.

The research was conducted in accordance with the Declaration of Helsinki. Informed consent was obtained from all participants after the goals of the study and consequences of participation had been discussed. The institutional review board of each institution involved in the study approved the research protocol. Further description of the Advanced Imaging for Glaucoma Study protocol can be found in the Advanced Imaging for Glaucoma Study Manual of Procedures (http://www.AIGStudy.net).

Optical Coherence Tomography Scanning Procedure

Both eyes of each participant were scanned with the Stratus OCT system. Data from the 2 scan patterns were analyzed. The first pattern was the fast macular thickness mapping (FMTM) scan, which consists of radial scans with a 6-mm scan length on 6 meridians centered on the fixation spot. The second scan pattern was the fast retinal nerve fiber layer scan, which acquires 3 consecutive circular scans of 3.4-mm diameter centered on the optic disc. To assess repeatability, 2 scans were obtained at the baseline visit. The raw data from FMTM scans were exported from the Stratus OCT system and analyzed with a computer program developed to measure automatically the thickness of retinal layers. The cpNFL thicknesses were computed by the Stratus OCT system using Stratus software version 4.0.

Image Processing

An automatic segmentation algorithm was developed to identify the boundaries between retinal layers. Figure 1A shows an OCT cross-sectional image along 1 radial line of the FMTM pattern. A Gaussian smoothing filter was applied to reduce speckle noise and to improve the signal-to-noise-ratio of the image. The intensity gradient was calculated for each OCT image. Searching from the

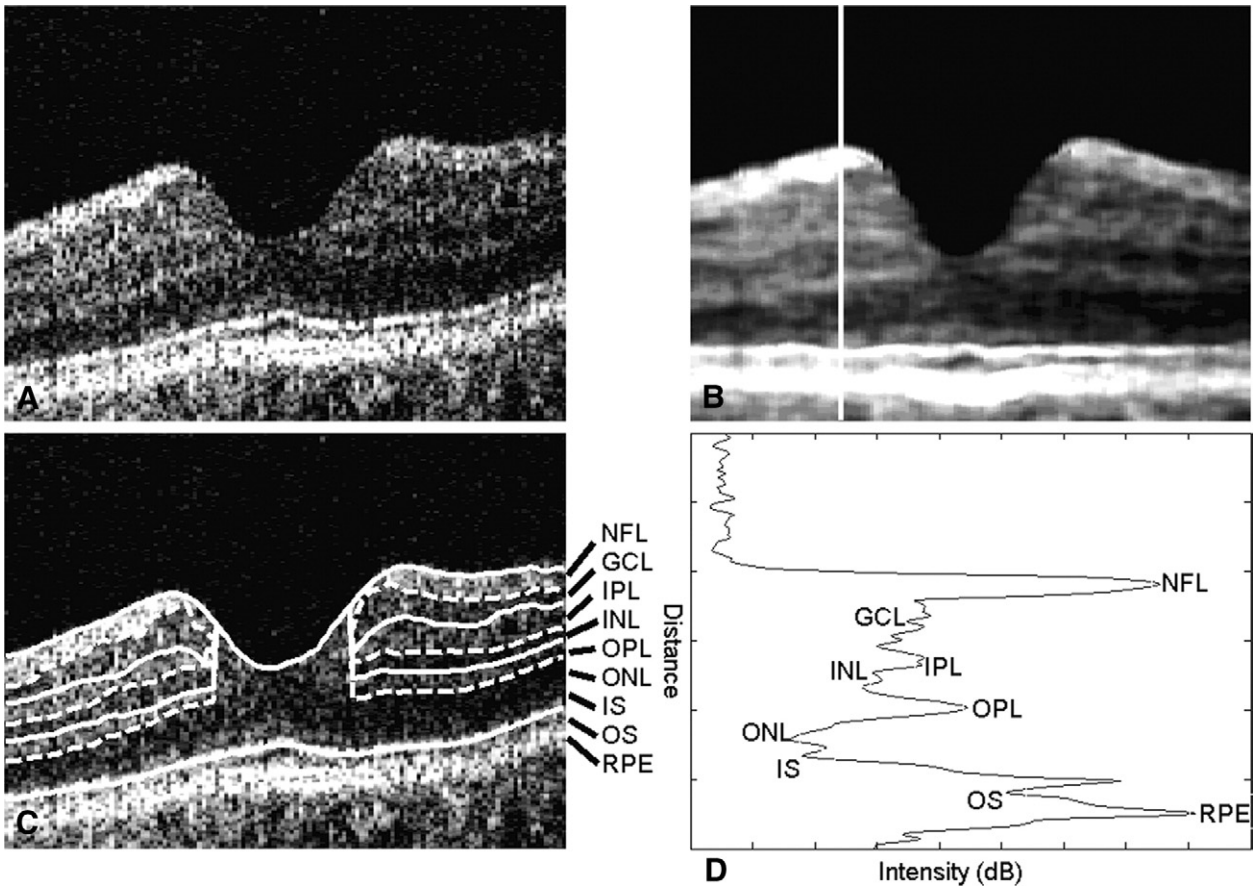

Figure 1. Steps in the segmentation of retinal layers. **A**, Raw optical coherence tomography (OCT) cross-sectional image of the macula. **B**, Image smoothed by a nonlinear diffusion filter. **C**, Boundary of retinal layers identified by the automated computer program. **D**, Axial scan from the parafoveal retina showing the layers. GCL = ganglion cell layer; INL = inner nuclear layer; IPL = inner plexiform layer; IS = photoreceptor inner segment; NFL = nerve fiber layer; OPL = outer plexiform layer; ONL = outer nuclear layer; OS = photoreceptor outer segment; RPE = retinal pigment epithelium.

inner to outer direction, the inner nerve fiber layer and the photoreceptor inner segment/outer segment junction (IS/OS) were identified, respectively, as the locations of the first and second largest gradient peaks. The distance between the inner macular NFL (mNFL) boundary and the IS/OS junction was considered to be the thickness of the entire retina. The image then was aligned according to the IS/OS junction. A nonlinear smoothing filter was applied to the aligned image for further smoothing and edge enhancement (Fig 1B). Figure 1D was the intensity profile of a single axial scan (A scan) from the filtered image (Fig 1B, white line). Based on the profile, it was possible to locate the macular nerve fiber layer (mNFL), the ganglion cell layer (mGCL), inner plexiform layer (mIPL), inner nuclear layer (mINL), and outer plexiform layer. The axial intensity gradient was calculated. The outer mNFL boundary, outer mIPL boundary, and outer plexiform layer boundary were identified as the 3 largest negative peaks between the inner mNFL boundary and the IS/OS junction on the gradient of the aligned image. The boundary between the mGCL and the mIPL was the most positive gradient peak within the zone demarcated by the outer limit of the mNFL and the outer limit of the mIPL. Figure 1C shows an overlay of the detected boundaries on the original OCT image. Because the inner retinal layers are absent in the fovea, a 1.5-mm diameter area centered on the fovea was excluded from later calculations.

To improve the accuracy of segmentation, a progressive refinement procedure was applied to extract the boundaries between layers. Progressive segmentation refers to an image processing technique whereby multiple nearby A-scan peaks are summed to increase the signal-to-noise ratio and to suppress speckle. The averaged A scan allows reliable boundary detection. Initially, all A scans along a radial line were averaged to obtain the overall average boundary locations. The cross-sectional image then was subdivided into several transverse regions and the A scans within each region were averaged. The boundaries identified on the overall average A scan then were used to guide the search for layer boundaries on the regional average A scans. The regional boundaries in turn were refined by subdividing the region into subregions. The procedure was applied iteratively until the layer boundaries were identified for each individual A scan. This progressive segmentation method improved reliability and reproducibility. When only individual A scans were segmented, wild deviations of boundary locations invariably occurred because of speckle noise. Whereas segmentation of averaged A scans excessively suppressed transverse variation in layer thicknesses, the progressive procedure improved reliability without sacrificing information on thickness variation.

After image processing, the boundary map was overlaid onto the original image for visual confirmation of boundaries. If apparent segmentation error was found, the scan was excluded from further analysis. The first scan was selected if both scans were segmented correctly. Otherwise, the scan with correct segmentation was selected. The repeatability study used both scans.

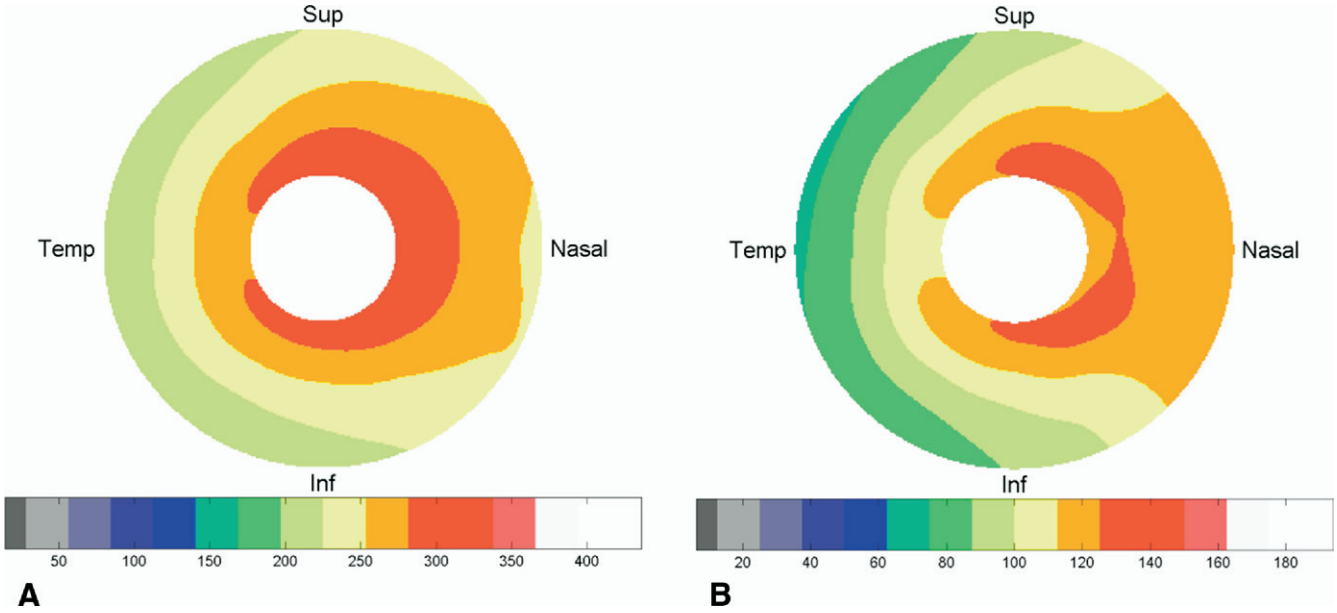

Figure 2. Average thickness maps in the normal group. **A**, Total retinal thickness. **B**, Inner retinal layer thickness. Inf = inferior; sup = superior; temp = temporal.

Feature Extraction

After boundaries were detected on OCT images with the FMTM scan, the thickness profiles of the 6 radial scans could be combined into a thickness map. Thin-plate spline interpolation was implemented in the mapping process. Thickness mapping was applied to the layers of interest: mNFL, mGCL, mIPL, and mINL. The thicknesses of several composite layers also were defined and measured: mGCL + mIPL, inner retinal layers (mIRL = mNFL + mGCL + mIPL, mIRL2 = mIRL1 + mINL), total retinal thickness (mRetina), and the outer retinal layer (mORL = mRetina − mIRL2). Area-weighted average thicknesses were calculated from the thickness maps, excluding the fovea (central 1.5-mm diameter). The normal reference was calculated by averaging measurements from eyes in the normal group. Figure 2 displays the population averaged thickness map of mRetina and mIRL. The fractional loss maps were calculated by subtracting the average mIRL thickness maps of PG and GSPPG eyes from the average normal mIRL thickness map and dividing the difference maps by the normal map. The Stratus OCT version 4.0 software was used to calculate and export average cpNFL thicknesses from the fast retinal nerve fiber layer scans.

Statistical Analyses

Because both eyes of each subject were used in the analyses, the standard errors of statistical tests were adjusted for the inter eye correlation. This was accomplished by the use of generalized estimating equations.[16] To assess discriminating power for glaucoma, areas under the receiver operating characteristic curve (AUCs) were calculated. The AUC estimates and their covariance matrix were calculated using the methods of DeLong et al[17] and Obuchowski,[18] and comparison between AUC values were adjusted for correlation between the 2 eyes of each subject and between algebraically related parameters. The AUC estimation procedure was written in MATLAB 7.0 (MathWorks, Natick, MA), and the other statistical analyses were carried out using SAS software version 9.1 (SAS Institute, Cary, NC). The study was based on hypothesis generation and the level of significance was set at 0.05.

Results

The initial group included a total of 167 participants (334 eyes). Sixty-one eyes were excluded because of visibly inaccurate segmentation boundaries. The resulting eligible 273 eyes from 149 participants (54 males and 95 females) were compared. The N group consisted of 93 eyes from 47 participants, aged 52±9 years (mean ± standard deviation [SD]). The GSPPG group included 55 eyes from 29 participants, aged 58±10 years. The PG group was made up of 125 eyes from 73 participants, aged 63±9 years. The age- and gender-related differences in macular thickness were not statistically significant for any layer except the mORL, which is significantly thicker in males than it is in females ($P = 0.006$). We combined glaucoma suspect and preperimetric glaucoma eyes because they had similar thicknesses of retinal layers (mIRL, mRetina, and cpNFL thickness did not differ significantly).

The GSPPG group had a VF MD of 0.13±0.98 dB, a PSD of 1.53±0.5 dB, IOP of 20.25±5.23 mmHg, and CCT of 571.09±38.99 μm. The PG group had an MD of −3.94±4.76 dB, a PSD of 5.62±4.29 dB, IOP of 15.10±3.72 mmHg, and CCT of 540.67±40.74 μm. Of the 125 eyes in the PG group, 96 eyes (76.8%) had an MD of −6.0 dB or more (early glaucoma), 17 eyes (13.6%) had an MD between −6.01 and −12.0 dB (moderate glaucoma), and 12 eyes (9.6%) had an MD of <−12 dB (advanced glaucoma).

Figure 2 shows the average mRetina and mIRL thickness maps of the N group. Both maps show increased thickness in the parafoveal ring and along the papillomacular NFL bundle. Table 1 shows the average macular thicknesses of the retinal layers in the 3 groups. Except for the mORL in the PG group, all layer thicknesses showed statistically significant thinning in the GSPPG and PG groups compared with the N group.

Repeatability of potentially useful glaucoma diagnostic parameters derived from macular scanning was assessed by 3 measures:

Table 1. Area-Weighted Average Retinal Layer Thickness in Normal, Glaucoma Suspect and Preperimetric Glaucoma, and Perimetric Glaucoma Eyes

	Normal Eyes		Glaucoma Suspect and Preperimetric Glaucoma Eyes			Perimetric Glaucoma Eyes		
	Mean (SD)	*Range*	*Mean (SD)*	*Range*	*P Value*	*Mean (SD)*	*Range*	*P Value*
mNFL	33.9 (5.1)	22.9–52.0	28.8 (3.4)	22–36.2	<0.0001	27.0 (5.4)	17.5–42.9	<0.0001
mGCL	34.9 (3.9)	24.7–45.6	32.4 (3.3)	25.5–42.0	0.0001	26.5 (4.7)	14.0–35.1	0.0001
mIPL	37.5 (4.1)	27.1–48.7	34.3 (3.8)	27.5–47.0	<0.0001	31.0 (3.8)	19.3–40	<0.0001
mINL	33.0 (3.2)	23.7–40.5	31.7 (2.6)	27.4–41.0	0.008	30.6 (2.5)	22.0–39.3	<0.0001
mGCL + mIPL	72.5 (7.2)	51.8–88.2	66.8 (6.3)	54.2–81.8	<0.0001	57.6 (8.1)	35.3–74.2	<0.0001
mIRL	106.3 (10.5)	79.1–137.2	95.6 (8.1)	77.2–118.0	<0.0001	84.6 (12.6)	54.9–110.8	<0.0001
mIRL2	139.3 (12.7)	102.8–173.8	127.2 (9.7)	107.5–149.4	<0.0001	115.2 (13.5)	77.5–144.5	<0.0001
mORL	113.3 (8.0)	96.2–130.7	110.7 (6.2)	100.6–131.4	0.040	110.1 (7.5)	92.2–129.5	0.0020
mRetina	252.6 (17.7)	204.7–299.2	237.9 (13.3)	209.0–273.3	<0.0001	225.3 (16.5)	183.7–256.2	<0.0001
cpNFL	101.7 (11.6)	73.6–135.1	87.7 (10.1)	65.5–107.5	<0.0001	74.4 (14.3)	40.2–108.2	<0.0001

cpNFL = circumpapillary nerve fiber layer thickness; mGCL = macular ganglion cell layer thickness; mIPL = macular inner plexiform layer thickness; mINL = macular inner nuclear layer thickness; mIRL = macular inner retinal layer thickness (mNFL + mGCL + mIPL); mIRL2 = macular inner retinal layer thickness 2 (mIRL + mINL); mNFL = macular nerve fiber layer thickness along a 6-mm diameter circle centered on the fovea; mORL = macular outer retinal thickness (mRetina − mIRL2); mRetina = total macular retinal thickness; SD = standard deviation.

pooled SD, coefficient of variation (CV) of repeated measures, and intraclass correlation coefficient (ICC; Table 2). The SD, based on absolute thickness, provided an indication of how well measurement can track progressive thinning resulting from glaucoma over time. The CV was measured as a fraction of the mean and provided an indication of how well measurement can track fractional tissue loss as a result of glaucoma over time. The data clearly show that combining individual inner retinal layers (mNFL, mGCL, mIPL) into composite layers (mGCL + mIPL, and mIRL) improved CV. The ICC, computed from a random effect model, is the ratio of intrasubject variance plus intereye variance to total variance. In the GSPPG and PG groups, it provided an indication of how finely a parameter can track progression through stages of the disease. Total retinal thickness had the best ICC, followed by mIRL thickness. The individual inner retinal layers did not perform as well in terms of ICC.

To find out which OCT parameters best differentiated the PG and GSPPG participants from the N participants, the fractional loss, SD, and AUC values were computed (Table 3). The fractional deviation was computed by dividing the deviation from the mean thickness in the N group (normal mean) by the normal mean. The standardized deviation was calculated by dividing the deviation from the normal mean by the population SD in the N group. The fractional deviation indicates which layer is most affected by glaucoma. Looking at the single layers, the mNFL, mGCL, and mIPL were heavily affected by glaucoma, with approximately 20% thinning in the PG group. The mINL was affected to a lesser degree, and the mORL was not affected by glaucoma at all. The fractional loss of mIRL thickness was significantly more severe than the mRetina in both PG ($P<0.0001$) and GSPPG ($P<0.0001$) groups by a generalized estimating equation-adjusted 2-sided *t* test.

The standardized deviation provides an indication of how well a parameter can differentiate eyes with glaucoma from the N group. The parameter may be more robust than the AUC when the sample size is limited. By this measure, mIRL is the best macular parameter, closely followed by mIRL2 and mGCL+mIPL. The standardized deviation of mIRL thickness was significantly greater than the mRetina in both the PG ($P<0.0001$) and GSPPG ($P = 0.005$) groups by a generalized estimating equation-adjusted 2-sided *t* test.

The AUC provides a direct measurement of discriminant power. The AUC for cpNFL and 3 macular thickness parameters, mIRL, mIRL2, and retina, were calculated because they performed best in terms of repeatability and standardized deviation. The mIRL was the macular parameter with the highest discriminant power. The mIRL measurement was better than mRetina in the PG group with borderline statistical significance ($P = 0.035$, 1-sided test). Although the AUC value for mIRL was still lower than cpNFL, the difference was not statistically significant in either the PG or GSPPG group.

Table 2. Measures of Repeatability

	Normal Eyes			Glaucoma Suspect and Preperimetric Glaucoma Eyes			Perimetric Glaucoma Eyes		
	SD	*CV*	*ICC*	*SD*	*CV*	*ICC*	*SD*	*CV*	*ICC*
mNFL	1.55	0.051	0.87	1.20	0.046	0.86	2.46	0.091	0.83
mGCL	2.29	0.061	0.76	1.89	0.056	0.70	1.95	0.077	0.93
mIPL	2.23	0.061	0.74	1.75	0.053	0.78	2.33	0.071	0.74
mGCL + mIPL	1.94	0.026	0.94	1.77	0.027	0.92	2.75	0.047	0.93
mIRL	2.51	0.024	0.95	1.95	0.021	0.95	1.48	0.017	0.99
mRetina	3.52	0.014	0.96	1.34	0.006	0.99	1.66	0.007	0.99

CV = coefficient of variation of repeated measures; ICC = intraclass correlation; mGCL = macular ganglion cell layer; mIPL = macular inner plexiform layer; mIRL = macular inner retinal layer; mNFL = macular nerve fiber layer; mRetina = macular total retinal thickness; SD = pooled standard deviation of repeated measures.

Table 3. Measures of Discriminant Power

	Fractional Deviation* ± SD		Standardized Deviation† ± SD		Area under the Receiver Operating Characteristic Curve ± SE	
	Glaucoma Suspect and Preperimetric Glaucoma Eyes	*Perimetric Glaucoma Eyes*	*Glaucoma Suspect and Preperimetric Glaucoma Eyes*	*Perimetric laucoma Eyes*	*Glaucoma Suspect and Preperimetric Glaucoma Eyes*	*Perimetric Glaucoma Eyes*
mNFL	−0.15±0.1	−0.20±0.16	−0.99±0.66	−1.33±1.05	—	—
mGCL	−0.07±0.09	−0.24±0.13	−0.64±0.84	−2.15±1.2	—	—
mIPL	−0.09±0.1	−0.17±0.1	−0.78±0.93	−1.58±0.92	—	—
mINL	−0.04±0.08	−0.07±0.08	−0.41±0.83	−0.74±0.79	—	—
mGCL + mIPL	−0.08±0.09	−0.21±0.11	−0.79±0.88	−2.07±1.12	—	—
mIRL	−0.10±0.08	−0.20±0.12	−1.02±0.77	−2.06±1.2	0.80±0.05	0.91±0.03
mIRL2	−0.09±0.07	−0.17±0.1	−0.95±0.77	−1.90±1.06	0.79±0.05	0.91±0.03
mORL	−0.02±0.05	−0.03±0.07	−0.33±0.78	−0.40±0.94	—	—
mRetina	−0.06±0.05	−0.11±0.07	−0.83±0.76	−1.54±0.94	0.75±0.06	0.87±0.03
cpNFL	−0.14±0.1	−0.27±0.14	−1.21±0.87	−2.36±1.23	0.82±0.05	0.94±0.02

cpNFL = circumpapillary nerve fiber layer thickness; mGCL = macular ganglion cell layer thickness; mIPL = macular inner plexiform layer thickness; mINL = macular inner nuclear layer thickness; mIRL = macular inner retinal layer thickness (mNFL + mGCL + mIPL); mIRL2 = macular inner retinal layer thickness 2 (mIRL + mINL); mNFL = macular nerve fiber layer thickness along a 6-mm-diameter circle centered on the fovea; mORL = macular outer retinal thickness (mRetina − mIRL2); mRetina = total macular retinal thickness; SD = standard deviation; SE = standard error.
—, not calculated.
*From the average value in the normal group expressed as a fraction of the normal average.
†From the normal average divided by the SD in the normal group.

The average fractional loss maps for the mIRL in the GSPPG and PG groups were calculated to identify the macular regions primarily affected by glaucoma (Fig 3). In the GSPPG group, the fractional loss was up to 20%. In the PG group, the fractional loss was up to 30%. In both groups, the loss was most pronounced in the inferior perifoveal region.

Discussion

Significant loss of retinal ganglion cells in the macular area has been shown in chronic experimental glaucoma in monkey eyes.[19,20] Direct measurement of the macular mGCL thickness theoretically would be a useful end point to detect

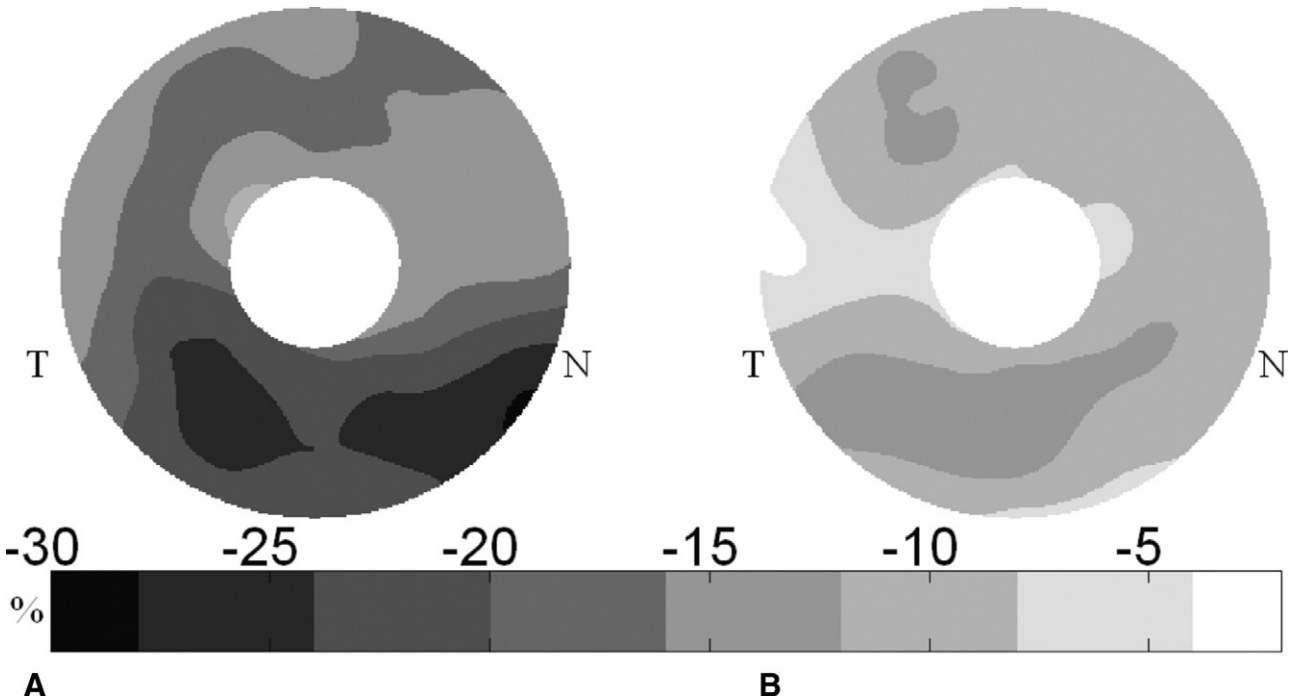

Figure 3. Pattern of inner retinal layer fractional loss map (unit, % thickness deviation from normal). **A**, Perimetric glaucoma group. **B**, Glaucoma suspect and preperimetric glaucoma group. N = nasal; T = temporal.

glaucoma. The current Stratus OCT software provides a map of mRetina along with regional averages, but it does not provide thickness measurements of retinal layers. Studies using the Stratus software have shown significant reductions in total macular thickness in glaucomatous eyes compared with normal eyes.[21–23] Software that segments retinal layers and measures the specific layers involved in glaucoma may improve glaucoma detection.

Leung et al[24] scanned the macula using the 3.45-mm diameter circular scan pattern (fast retinal nerve fiber layer pattern on Stratus OCT) and evaluated mNFL thinning in glaucoma. They showed significant overall thinning of the mNFL in glaucomatous eyes compared with normal eyes. In glaucoma suspect eyes, the mean mNFL thickness was not significantly thinner than that in normal eyes. However, when divided into sectors, the inferior (6:00) mNFL of glaucoma suspect eyes was significantly thinner than that of normal eyes.

Ishikawa et al[15] developed a macular segmentation algorithm to measure sublayer thickness for glaucoma diagnosis. They combined layers to minimize the variability of detected borders between individual layers. They showed that mNFL, inner retinal complex (IRC = mGCL + mIPL + mINL), and mRetina are thinner in eyes with perimetric glaucoma. The outer retinal layers were not found to be involved in glaucoma. Furthermore, the discriminating power of the 4 innermost retinal layers (mNFL + IRC) for glaucoma was significantly greater than the discriminating power of the mRetina. When the discriminating powers of the cpNFL and the combined 4 innermost retinal layers were compared, there was no significant difference.

These findings confirmed that glaucomatous macular thinning occurred primarily in the 3 innermost retinal layers (mNFL, mGCL, and mIPL), and to a lesser extent in mINL and only minimally in the outer retinal layers. This study included glaucoma suspects and preperimetric glaucoma participants and showed that macular thinning could be detected in all 4 macular inner retinal layers before VF loss. These results provide the strongest evidence so far that macular thinning within the inner retinal layers precedes VF changes in glaucoma. This is consistent with previous results showing that anatomic changes precede functional changes. It is know already that glaucomatous cpNFL loss precedes functional loss by as much as 5 years.[25] Optic disc changes also are known to precede visual field loss.[26] Previous research using enucleated human eyes with glaucoma showed that a 20% loss of retinal ganglion cells throughout the central 30° of the retina was associated with 5-dB sensitivity loss on automated perimetry.[27] These results showed 10% thinning of mIRL in the GSPPG group and 20% thinning in the PG group. Thus, these data indicate that the threshold of detectable VF loss occurs after a roughly 10% to 20% loss of thickness in the 3 inner retinal layers associated with ganglion cell components.

One weakness of these data is that glaucoma suspects and subjects with preperimetric glaucoma were combined into 1 group for data analysis. Some of the glaucoma suspects had high IOP, which can cause structural changes in the optic nerve and nerve fiber layer that do not represent ganglion cell loss. Thus, eyes may have been included in which the mIRL thinning was not the result of loss of tissue but rather of compression from the elevated IOP in those eyes.

The repeatability of thickness measurements for various retinal layers was investigated. Parameters with better repeatability in terms of SD and CV may perform better in the long-term tracking of glaucoma progression in an individual. Parameters with better ICC in the GSPPG and PG groups may work best for tracking disease progression. In terms of SD, no clear trend was detected as to which retinal layer performs better in terms of SD. Because the mIRL is only a fraction of the mRetina, the authors believed the repeatability in terms of SD would be better. However, this was true only for the N group and PG group, and not for the GSPPG groups. This may be the result of the sharper signal gradients at the inner and outer retinal boundaries. This indicates that the uncertainty of boundary delineation is roughly equal for the retinal layers analyzed. Combining the 3 inner retinal layers most affected by glaucoma into the mIRL would improve the repeatability of thickness measurements in terms of CV and ICC. Compared with mIRL thickness, the mRetina had a comparable SD and better ICC (it would be unfair to compare CV because mRetina includes the mORL, which is not affected by glaucoma). Overall, these results support the use of both mRetina and mIRL for tracking glaucoma progression.

The authors hypothesized that measuring the combined thickness of the retinal layers most affected by glaucoma would provide the best diagnostic parameters. The 3 innermost layers (mNFL, mGCL, and mIPL) are affected most severely by glaucoma, and the mIPL provides a relatively well-defined outer boundary; therefore, combining these 3 layers into an entity called the inner retinal layer seems to be a good strategy. The mINL is the fourth innermost layer and is affected by glaucoma to a moderate degree. This makes sense anatomically because the ganglion cell dendrites, soma, and axons reside in the 3 innermost retinal layers and the mINL would be affected by ganglion cell loss in glaucoma only secondarily. It is not clear whether including mINL thickness in a diagnostic parameter adds diagnostic power. To address this question, an alternative definition was tested, mIRL2, that included the 4 innermost retinal layers. Indeed, mIRL2 performed worse than mIRL. The difference was statistically significant in terms of fractional deviation ($P<0.0001$ for the PG and GSPPG groups) and standardized deviation ($P<0.0001$ for the PG group and $P = 0.04$ for GSPPG group), but not AUC. The mIRL was significantly better than the mRetina by all measures of discriminant power. These findings support measuring the thickness of the 3 innermost retinal layers (mIRL) to optimize glaucoma diagnosis with OCT macular mapping. But the alternative of using the 4 innermost layers would perform nearly as well.

Current clinical use of OCT for glaucoma diagnosis emphasizes cpNFL measurements because it has been shown to outperform macular retinal thickness as a diagnostic parameter.[9,11,28] The authors found that the diagnostic power of mIRL was comparable with that of cpNFL. This agrees with the findings of Ishikawa et al,[15] who also found that the thickness of the innermost layers in the macula had diagnostic power comparable with that of cpNFL.

The fractional loss maps showed that glaucomatous damage is most severe in the inferior perifoveal region that

partially overlaps the boundary of the 6-mm diameter scan pattern used for macular mapping on the Stratus OCT. This suggests that further improvements in diagnostic power may be achieved by increasing the diameter of the macular scanning area. The current Stratus OCT software maps the macula using 6 radial lines centered on fixation. This pattern has higher sampling density in the fovea, which does not contain the 3 inner retinal layers, and leaves large gaps in the peripheral macula, where the effect of glaucoma is most severe. Simple trigonometry shows that the gap is more than 1.5 mm between meridians at the outer edge of the 6-mm-diameter circular map. Thus, a scan pattern that samples more points in the periphery of the macula may provide more information on glaucomatous change. Based on these principles, the authors designed a new scan pattern, macular grid 7 (MG7), that evenly samples the macula over a 7-mm diameter circle. The center of the MG7 protocol is shifted 0.75 mm temporally to improve sampling of the temporal periphery. The MG7 patter consists of 768 A scans, the same number used in FMTM, and also takes 2 seconds to acquire using the Stratus OCT. The MG7 is being evaluated as part of the Advanced Imaging for Glaucoma Study, and the findings will be published in a later report.

In summary, the authors have confirmed that glaucoma primarily affects the thickness of the inner retinal layers in the macula, including mNFL, mGCL, mIPL, and, to a lesser extent, mINL. The combination of the 3 innermost retinal layers (mIRL) is comparable with the cpNFL in diagnostic power. Glaucoma predominantly affects the inferior periphery of the macula. A new OCT macular scanning pattern that increases the sampling of the peripheral macula may improve further the diagnostic performance of mIRL thickness. With further development, macular mapping with OCT may provide valuable and complementary anatomic information to be used together with the evaluation of optic nerve head and cpNFL in the diagnosis of glaucoma.

References

1. Hoyt WF, Newman NM. The earliest observable defect in glaucoma? Lancet 1972;1:692–3.
2. Sommer A, Pollack I, Maumenee AE. Optic disc parameters and onset of glaucomatous field loss. I. Methods and progressive changes in disc morphology. Arch Ophthalmol 1979;97:1444–8.
3. Funk J. Early detection of glaucoma by longitudinal monitoring of the optic disc structure. Graefes Arch Clin Exp Ophthalmol 1991;229:57–61.
4. Motolko M, Drance SM. Features of the optic disc in preglaucomatous eyes. Arch Ophthalmol 1981;99:1992–4.
5. Schubert HD. Anatomy and physiology: structure and function of the neural retina. In: Yanoff M, Duker JS, eds. Ophthalmology. London: Mosby; 1999:8.1.3.
6. Curcio CA, Allen KA. Topography of ganglion cells in human retina. J Comp Neurol 1990;300:5–25.
7. Asrani S, Zou S, d'Anna S, et al. Noninvasive mapping of the normal retinal thickness at the posterior pole. Ophthalmology 1999;106:269–73.
8. Bagga H, Greenfield DS. Quantitative assessment of structural damage in eyes with localized visual field abnormalities. Am J Ophthalmol 2004;137:797–805.
9. Guedes V, Schuman JS, Hertzmark E, et al. Optical coherence tomography measurement of macular and nerve fiber layer thickness in normal and glaucomatous human eyes. Ophthalmology 2003;110:177–89.
10. Wollstein G, Garway-Heath DF, Fontana L, Hitchings RA. Identifying early glaucomatous changes: comparison between expert clinical assessment of optic disc photographs and confocal scanning ophthalmoscopy. Ophthalmology 2000;107:2272–7.
11. Medeiros FA, Zangwill LM, Bowd C, et al. Evaluation of retinal nerve fiber layer, optic nerve head, and macular thickness measurements for glaucoma detection using optical coherence tomography. Am J Ophthalmol 2005;139:44–55.
12. Asrani S, Zeimer R. Retinal thickness analyzer. In: Huang D, Kaiser PK, Lowder CY, Traboulsi EI, eds. Retinal Imaging. Philadelphia: Mosby; 2006:111–24.
13. Huang D, Tan O, Fujimoto J, et al. Optical coherence tomography. In: Huang D, Kaiser PK, Lowder CY, Traboulsi EI, eds. Retinal Imaging. Philadelphia: Mosby; 2006:47–65.
14. Drexler W, Morgner U, Ghanta RK, et al. Ultrahigh-resolution ophthalmic optical coherence tomography. Nat Med 2001;7:502–7.
15. Ishikawa H, Stein DM, Wollstein G, et al. Macular segmentation with optical coherence tomography. Invest Ophthalmol Vis Sci 2005;46:2012–7.
16. Liang KY, Zeger SL. Longitudinal data analysis using generalized linear models. Biometrika 1986;73:13–22.
17. DeLong ER, DeLong DM, Clarke-Pearson DL. Comparing the areas under two or more correlated receiver operating characteristic curves: a nonparametric approach. Biometrics 1988;44:837–45.
18. Obuchowski NA. Nonparametric analysis of clustered ROC curve data. Biometrics 1997;53:567–78.
19. Glovinsky Y, Quigley HA, Pease ME. Foveal ganglion cell loss is size dependent in experimental glaucoma. Invest Ophthalmol Vis Sci 1993;34:395–400.
20. Frishman LJ, Shen FF, Du L, et al. The scotopic electroretinogram of macaque after retinal ganglion cell loss from experimental glaucoma. Invest Ophthalmol Vis Sci 1996;37:125–41.
21. Tanito M, Itai N, Ohira A, Chihara E. Reduction of posterior pole retinal thickness in glaucoma using the Retinal Thickness Analyzer. Ophthalmology 2004;111:265–75.
22. Greenfield DS, Bagga H, Knighton RW. Macular thickness changes in glaucomatous optic neuropathy detected using optical coherence tomography. Arch Ophthalmol 2003;121:41–6.
23. Lederer DE, Schuman JS, Hertzmark E, et al. Analysis of macular volume in normal and glaucomatous eyes using optical coherence tomography. Am J Ophthalmol 2003;135:838–43.
24. Leung CK, Chan WM, Yung WH, et al. Comparison of macular and peripapillary measurements for the detection of glaucoma. An optical coherence study. Ophthalmology 2005;112:391–400.
25. Sommer A, Katz J, Quigley HA, et al. Clinically detectable nerve fiber atrophy precedes the onset of glaucomatous field loss. Arch Ophthalmol 1991;109:77–83.
26. Zeyen TG, Caprioli J. Progression of disc and field damage in early glaucoma. Arch Ophthalmol 1993;111:62–5.
27. Quigley HA, Addicks EM, Green WR. Optic nerve damage in human glaucoma. III. Quantitative correlation of nerve fiber loss and visual field defect in glaucoma, ischemic neuropathy, papilledema, and toxic neuropathy. Arch Ophthalmol 1982;100:135–46.
28. Wassle H, Grunert U, Rohrenbeck J, Boycott BB. Cortical magnification factor and the ganglion cell density of the primate retina. Nature 1989;341:643–6.